Cement and Concrete Research 41 (2011) 1310–1319

Contents lists available at ScienceDirect

Cement and Concrete Research

journal homepage: http://ees.elsevier.com/CEMCON/default.asp

Long-term deformational simulation of PC bridges based on the thermo-hygro model of micro-pores in cementitious composites

Koichi Maekawa *, Nobuhiro Chijiwa, Tetsuya Ishida

Department of Civil Engineering, The University of Tokyo, Japan

ARTICLE INFO

Article history:
Received 17 November 2010
Accepted 29 March 2011

Keywords:
Multi-scale modeling
Moisture migration
Nonlinear creep
Environmental conditions
Excess deflection
Drying shrinkage

ABSTRACT

Creep deflections that greatly exceed the predicted values by the linear creep law are being found in measurements on actual PC bridge viaducts. In this study, structural creep deformations were reproduced by using the multi-scale coupled thermo-hygro and mechanical modeling which enables to deal with an interaction of chemo-physical events of differing dimensions ranging from the kinematics of moisture in micro-pores to the macroscopic structural mechanics, and the effect of various factors was analytically investigated. The numerical analysis approximately reproduced the excessive deflection measured on an actual bridge viaduct. It was confirmed that the creep bending of the viaduct having the hollow cross-section varies significantly due to the ambient temperature, humidity and the structural specific surface area. The macroscopic structural responses in association with the thermodynamic state of moisture in the micro-pores are also discussed.

1. Introduction

In all parts of the world, excessive deflection that greatly exceeds the design values has been reported for PC bridge viaducts that have been constructed for more than 20 years [1–4]. Most of these bridges were constructed around 1975 and were designed in use of the linear creep law that assumes the evolution of creep strains 2–3 times the elastic strains. However, back calculating from the actual deflection on the bridge viaducts, the linear creep coefficient of around 4–5 is inversely obtained [5,6], which is more than double the value measured in laboratories and used in design guides of each country [7–9]. Although creep and drying shrinkage of concrete specimens can be estimated with high accuracy, there is much scope for improvement in the prediction of long term deformation of actual structures. For the maintenance management of existing PC bridges, it is essential to be able to determine whether the long term flexure will converge or not, as well as when and to what value, based on scientific grounds.

The apparent creep of concrete specimens depends on the micro-pore structure of the hardened cement paste and the thermodynamic state of moisture trapped in the pores. Hardened cement paste is formed as a collection of pores of various sizes, ranging from relatively coarse capillary pores to interlayer pores on the scale of water molecules. The kinematics of moisture in micro-pores and the deformational behavior of cement hydrates that form gel and capillary pores vary greatly depending on the scale of the pores. To construct a time-dependent deformational model of cementitious composites, it is necessary to take into account the different deformational characteristics of each of the microstructural units.

The authors have developed a 3-dimensional material–structure coupled analysis (abbreviated as *DuCOM-COM3*) [10] that tracks the time history of the variation in long term properties of concrete structures from production stages to the end of its service life. By running in parallel a thermodynamic coupled analysis that numerically models hydration reactions, pore structure formation, moisture migration in a coupled manner (nm to μm), and a material–structure response analysis (mm to meter scale) based on a nonlinear material constitutive law while sharing digital information successively, it is possible to follow the phenomena (Fig. 1). By integrating the phenomena of moisture movement and solid–liquid equilibrium within micro-pores of different dimensions, a constitutive model that can be applied to volumes ranging from “cm” to “meter” scales can be constructed [11,12]. It is possible to evaluate macroscopic structural deformation or cracking damage, etc., caused by the phenomena at the scale of water molecule, such as internal stresses due to capillary tension or surface energy. The moisture transport through micro-pores of cement hydrates is simulated in terms of the vapor diffusion and the convection of condensed water [10,31] as shown in Fig. 1.

Here, the vapor pressure as the primary variable for the molecular diffusion is computed so as to satisfy the thermodynamic equilibrium with the condensed water stored in micro-pores with non-uniform pore-size distribution. After the cracking in structural concrete, the moisture transport is accelerated since the additional paths surrounded by crack planes are created. This coupling effect of the structural damage on the micro-thermodynamics is automatically

* Corresponding author. Fax: +81 3 5841 6010.
E-mail address: Maekawa@concrete.t.u-tokyo.ac.jp (K. Maekawa).

0008-8846/$ – see front matter © 2011 Elsevier Ltd. All rights reserved.
doi:10.1016/j.cemconres.2011.03.021

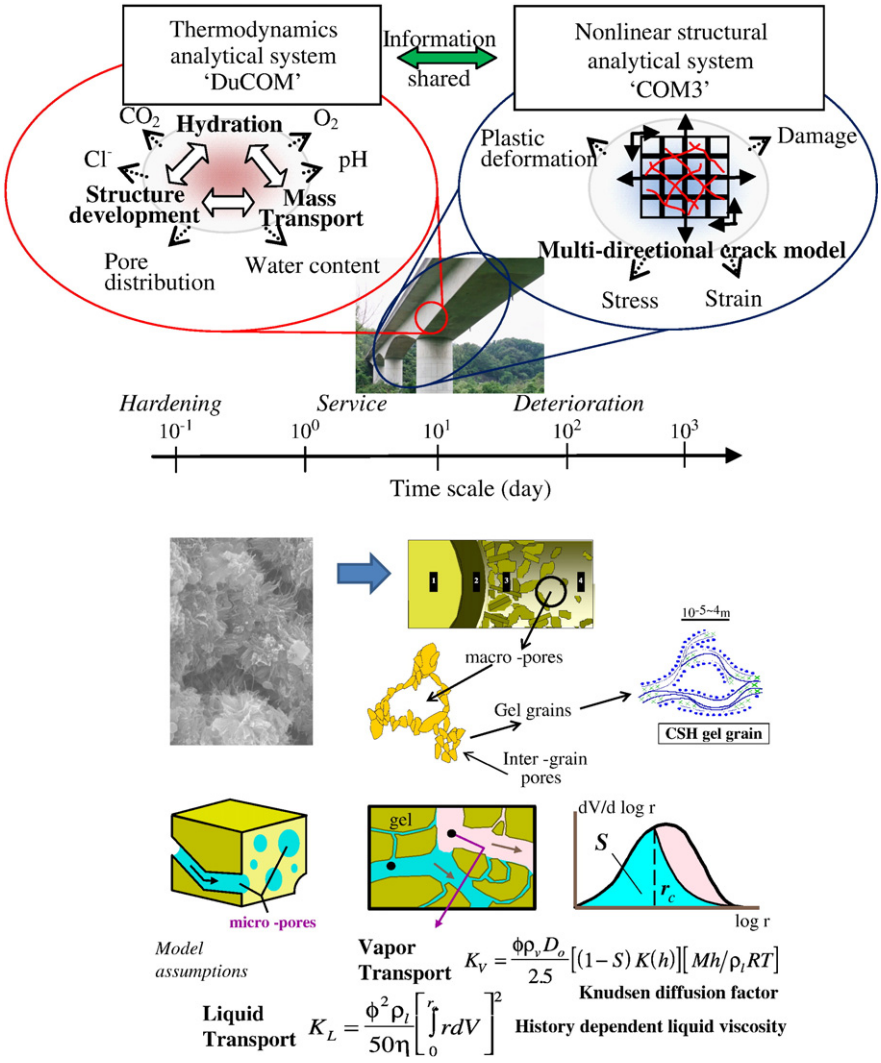

Fig. 1. Outline of multi-scale integrated analytical system [10,31].

taken into account as the crack spaces are mathematically treated as newly created large-scale pores, whose size is equal to the crack spacing computed by the linked structural analysis of COM3 [32]. In other words, the formed pore structure in concrete is governed by both cement hydration and mechanical cracking [33].

This study uses the numerical simulation that couples material science and structural mechanics to examine the causes of excessive long term creep deflection observed in an actual bridge to validate the model. By carrying out sensitivity analyses in which the behavioral model in micro-pores is intentionally changed, a quantitative discussion on the thermodynamic state of moisture at the microscopic level and macroscopic structural responses is performed, with the objective of deepening our understanding on structural creep.

Table 1
Composition of the hardened concrete.

σ_{ck}	Cement	Max. gravel size	Air
MPa	Class	mm	%
40	Early-strength cement	25	4

Mix proportion of concrete (kg/m^3)					Remarks
Cement	Water	Sand	Gravel	Admixture	
423	165	639	1108	1.0575	Summer
440	167	629	1099	1.1	Other seasons

2. Tsukiyono Bridge viaducts

2.1. Target structure in detail

The subject of the analysis is Tsukiyono Bridge in Japan, which was completed in 1982 and for which the measured deflection at the span center has been reported [1,5,6,13]. For this bridge, the design drawings, details of materials used, the records of the construction procedures, and the monitoring results after construction have been preserved in detail and published. This is widely regarded as valuable data that can withstand scientific analysis. The bridge is a 4-span PC hinged moment-resisting frame constructed by the Polensky & Zöllner method (P&Z method). Concrete was cast in divided blocks, and after prestressing, the next block was consequently constructed. The specification of concrete used is shown in Table 1.

This study covers the span from pier P4 to pier P5, the area from the support point at pier P4 side to the center of the span (Fig. 2). In this area strain gages were embedded in concrete at the time of concreting works. Then, it is possible to refer to the actually measured data of drying shrinkage of volume. The bridge girder cross-section has a hollow shape, with a top flange that includes the bridge parapets 10.65 m wide, and a bottom flange of 5.8 m wide. The top flange

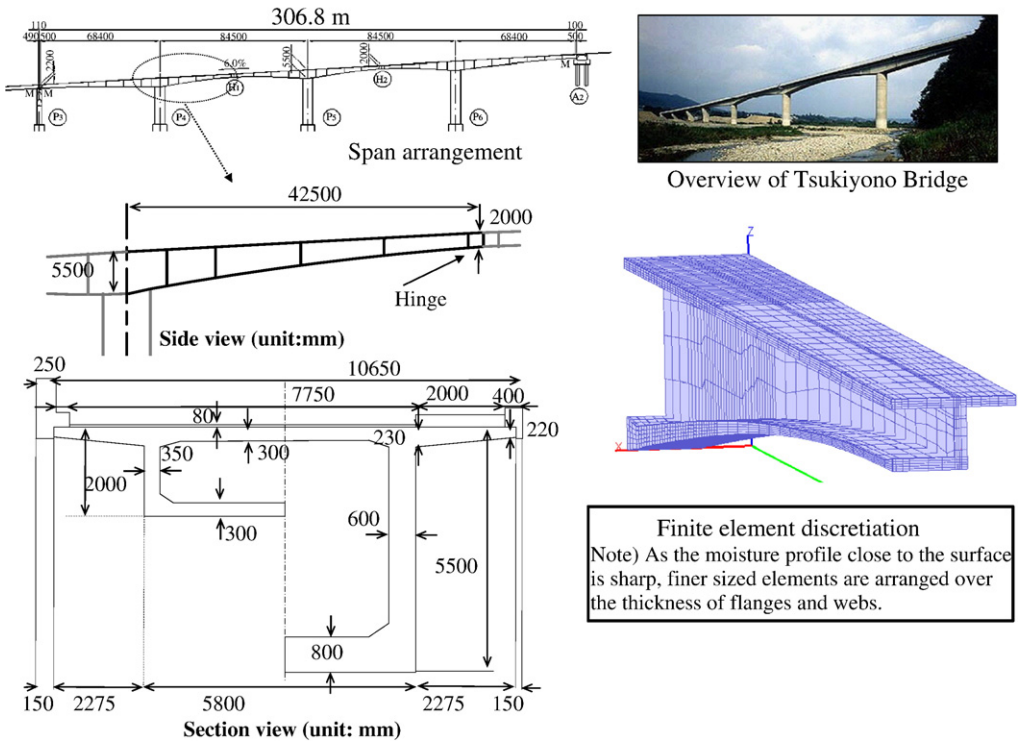

Fig. 2. Tsukiyono Bridge at the location to be analyzed.

thickness is uniform at 300 mm (excluding the thickness 80 mm of road paving), but the web thickness varies between 600 mm and 360 mm, and the bottom flange thickness varies between 754 mm and 200 mm, varying continuously from the support point to the hinge at the center span. As shown in Fig. 2, the six blocks were constructed in-situ while extending outwards. The construction period was from July (beginning of summer) to September, then after 1250 days had passed, the road pavement was laid. After casting concrete to the main structure, curing was carried out for 3 days in a sealed condition, on the following day, PC cables were tensioned, then on the sixth day, the P&Z device was moved, completing one block in a cycle of 10 days.

The local temperatures were obtained from the meteorological data near the construction site [12] and the relative humidity was estimated by the data from Karuizawa meteorological station, which is considered to have topographical conditions close to those of Tsukiyono area as shown in Table 2. The annual average temperature was 10.2 °C and relative humidity 78%.

2.2. Creep deflection measured in the past decades

Fig. 3 shows the variation with time of the vertical deflection at the span center, measured by an optical measurement device since completion of construction in 1982. Departure from the prediction by the linear creep law started a few hundred days after completion of the bridge. The deflection by the linear creep law was calculated by the superposition method of specific creep and the normal creep coefficient of 1.58, which was specified in the design code for practice. The concrete compressive strength of 40 MPa, Young's modulus of 35 GPa, relative humidity of 70%, volume to surface area ratio of 40 cm and drying shrinkage of 185 μ were used in the calculation at design.

Table 2
Local temperature and humidity patterns.

Month	Jan.	Feb.	Mar.	Apr.	May.	Jun.
T (°C)	−1	−1	2	8	14	18
RH (%)	73	72	71	70	74	81
Month	Jul.	Aug.	Sep.	Oct.	Nov.	Dec.
T (°C)	21	23	19	12	6	1
RH (%)	85	85	88	83	77	73

3. Coupled multi-scale chemo-physical and structural analysis

In order to analyze the creep deflection of Tsukiyono Bridge as described in Section 2, the 3-dimensional coupled material–structural analysis system was applied as described in Section 1. This takes into account the mutual interaction of thermodynamic phenomena at various scales, from the kinematics of water molecules in hardened cement paste to the deformation at the structural level. By just inputting the concrete mix proportion, construction conditions, structural parameters (dimensions, shape, and reinforcement arrangement), the loads and ambient conditions, thermodynamic

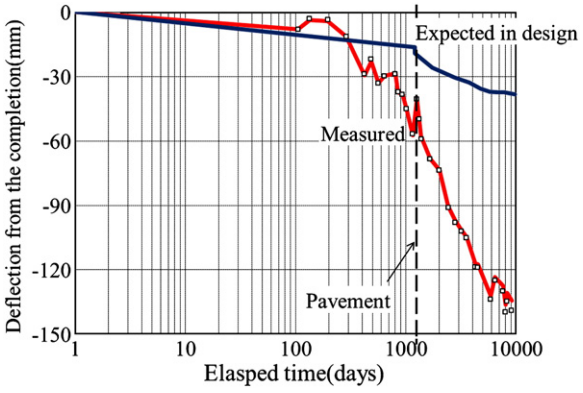

Fig. 3. Difference in predicted and measured values of deflection (the component caused by the overlaid pavement is taken out from the entire deflection).

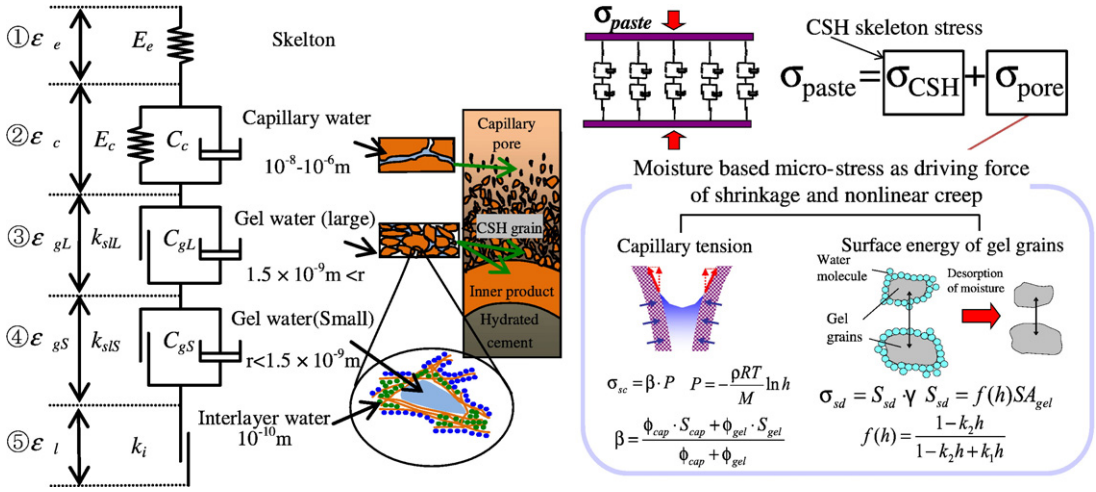

Fig. 4. Multi-scale moisture-based creep model.

quantities represented by hydrates and water content are successively calculated, and the macroscopic deformational behavior of the structure is calculated with the following time-dependent constitutive law. It is known from the site-investigation that there is no visible cracking in the viaduct. Then, the nonlinear coupling effect of cracking and moisture transport has no impact in this study.

3.1. Multi-scale time-dependent constitutive law

The multi-scale time-dependent constitutive law [10–12] incorporated into the analysis consists of a mechanical model in accordance with the dimensions and form of the micro-pore structures together with the state of the moisture in the pores, that overall can express the macroscopic time-dependency of hardened concrete. The elastic response of the hardened cement hydrates is represented by the elastic model as indicated by component (1) in Fig. 4. The constituent element associated with the state of the capillary water in the comparatively large pores in the scale 10^{-6}m to 10^{-8}m is shown by component (2), a visco-elastic model that represents the relatively quick response. This term plays a dominant role on the creep at the initial loading \period. The moisture in gel pores corresponding to the space 10^{-8}m–10^{-9}m in components (3) and (4) is considered to be in steady motion due to the molecular interaction from the solid wall surfaces. This is thought to contribute to the component of unrecoverable plastic deformation, and for which a visco-plastic model is applied. This term contributes to the progress of creep over a comparatively long time as indicated by (2). In the interlayer pores at the 10^{-10} m scale, the pores are sufficiently small. Then, water molecules passes through the pores, and the pores are blocked by the increase in surface energy. So, this is represented by a plastic model only as in (5). This model is associated with deformation under conditions where the evaporation of water is significant, such as under high temperatures or low humidity.

The progressing hydration and associated increase in stiffness are computationally expressed by adding the spring–dash pot components as shown in Fig. 4. In this composite system of cement paste phase, moisture related stress components are overlaid, that is, the capillary water pressure and disjoining pressure as shown in Fig. 4. Then, the effect of drying associated with the moisture migration and self-desiccation by the loss of free water can be automatically considered [9,10] in the scheme of multi-scale, multi-component and multi-phase modeling. This formulated cement paste modeling is combined with the elastic solids of aggregates to form the system of concrete. To date, this constitutive model has been validated by using concrete specimens in laboratory tests. Detailed verification was carried out for autogenous and drying shrinkage, basic and drying creep under various humidity and load conditions [7].

3.2. Element discretization

Near the surface of a structure exposed to the ambient conditions, the local gradient of the enthalpy and the pore water pressure become large. In order to ensure the analytical accuracy of this part, discretized finite elements with dimensions in the order of [mm] were set near the structural surface. As the gradient of temperature and humidity around the core of members is comparatively small, element dimensions in the order of several [cm] were set in the center. The finite element dimension in the direction of the bridge axis could be allowed to be up to several meters, considering that the bending moment acting in the longitudinal direction has a linear distribution, and the variation in the thermodynamic state quantities is actually small.

3.3. Computational conditions

The numerical analysis was carried out in accordance with the construction sequence of casting fresh concrete in stages. After form stripping, the gravity load was applied on the whole structure. The road pavement and the weight of parapets were input as distributed loads acting on the top flange, which acted starting 1250 days after completion of the main structure. The time of completion of the main structure was taken to be the origin, and thereafter the elapsed time and amount of increase in deflection were recorded. The relationship between deflection and elapsed time in the analysis in accordance

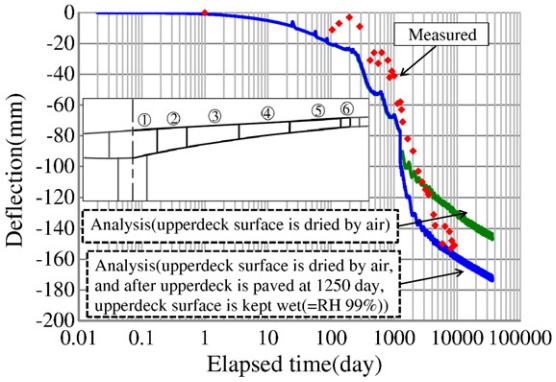

Fig. 5. Analyzed creep deflection of Tsukiyono Bridge (up to 100 years: the effect of overlay pavement is included in both analysis and the measurement.).

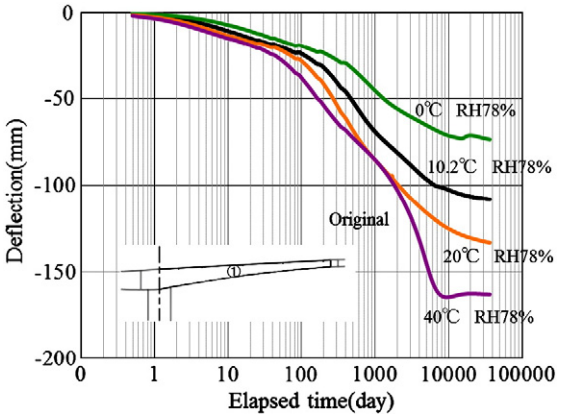

Fig. 6. Variation in the deflection with time for temperature assumed to be constant.

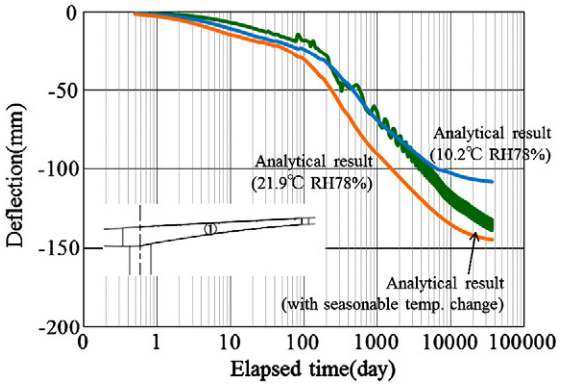

Fig. 7. Variation in the deflection with time for temperature assumed to fluctuate.

with this definition is shown in a later chapter. The external air conditions were assumed to vary monthly using the values as shown in Table 2 [14], and the concrete initial temperature at the time of casting was taken to be 20 °C. The environmental conditions were assumed to be the same inside and outside the box girder as well as on the bottom surface, and it was assumed that the top flange of the box girder was exposed to drying due to the external air, both before and after the pavement was laid. Since the pavement may play a role to wrap the concrete top flange as well, the exposure to the wet atmosphere as RH = 99% after the pavement was set forth as an extreme case for discussion.

3.4. Reproduction of the long term creep deflections

The analysis results were similar to the deflections measured on the bridge for both short and long terms after construction (Fig. 5). In the actual measurements, the rate of creep deflection is accelerated after about 1000 days. The analysis also reproduces the same behavior, and the reality is caught in between the two analyses results of both extreme exposure conditions. In the period from several tens to several hundreds of days, a certain amount of difference can be seen in the rate of progressing deflection between the analytical and the measured values. During this period, the top road surface was not paved. So, it was exposed to the radiation of sun shine. Then, it is considered that the top flange of the bridge was locally placed under higher temperatures and drying conditions than assumed in the analysis. It is predicted that the deflection of Tsukiyono Bridge will gradually increase and settle down to about 140–180 mm deflection at 100 years after construction. Then, in order to verify the whole system of prediction, the authors propose not to terminate the long-term monitoring but continue another 50 years of site-investigation.

4. Influencing factors on the creep deformation

It has been confirmed that it is possible to approximately reproduce the excessive deflection occurring in the real bridge. In this chapter, a sensitivity analysis is carried out on the effect of temperature, humidity and volume to surface area ratio of the girder. The mechanism of the excessive deflection is investigated. Here, in order to clarify the effect of the influencing factors, the complexity of the construction process was eliminated, that is to say, the bridge including the pavement and the parapets is constructed at once, and prestressed through PC strands at the same time. The prestressing force and other loads all act at the origin of the time and deflection. The environmental conditions inside and outside the box girder and at the bottom surface are all the same.

4.1. Sensitivity of ambient temperature

Two conditions were investigated: the ambient temperature constant throughout the year, and fluctuating according to the seasons. For the constant temperature analysis, the external temperature was set to 0 °C, 10.2 °C, 20 °C, and 40 °C, and the humidity of the external air was set to an annual average of 78%. As shown in Fig. 6, the analysis results show that the higher the temperature is, the greater the final value of deflection. As the temperature increases, the concrete shrinkage increases. And movement of moisture in the pores is accelerated. This results in increased creep deformation.

The analysis results corresponding to the varying temperature (Table 3) and the annual average humidity (kept constant at 78%) are shown in Fig. 7. The analysis results are also shown for constant annual average temperatures of 10.2 °C and 21.9 °C, which are the highest temperatures in the fluctuating range as shown in Table 3. The deflection varies at a rate close to those of the analyses carried out with constant annual average temperature, and it converges to a final value close to the analytical one under the highest temperature. This can be explained by irreversible creep occurring during high temperature periods. The difference of the analysis result in Fig. 5 from that of Fig. 7 is less than 2 cm. It means that the block construction procedure cannot be a primary factor of the excessive deflection.

4.2. Sensitivity of ambient relative humidity

Two cases were investigated with the annual average temperature held constant at 10.2 °C: different relative humidities held constant throughout the analysis, and the relative humidity fluctuating throughout the year as shown in Table 4. In the analyses with constant relative humidity, values of 99%, 78%, 60% and 30% were assumed. The lower the relative humidity is, the greater the deflection

Table 3
Temperature seasonal fluctuation pattern.

No. of days elapsed	45	91.25	136.25	182.5
External air temperature (°C)	−1.17	0.97	10	16.4
No. of days elapsed (contd.)	227.5	273.25	318.25	365
External air temperature (°C)	21.9	20	10.4	3.2

Table 4
Seasonal fluctuation pattern of relative humidity.

Time in 1 cycle	45	91.25	136.25	182.5
RH (%)	73	73	76	76
Time in 1 cycle	227.5	273.25	318.25	365
RH (%)	86.7	87.3	81	75

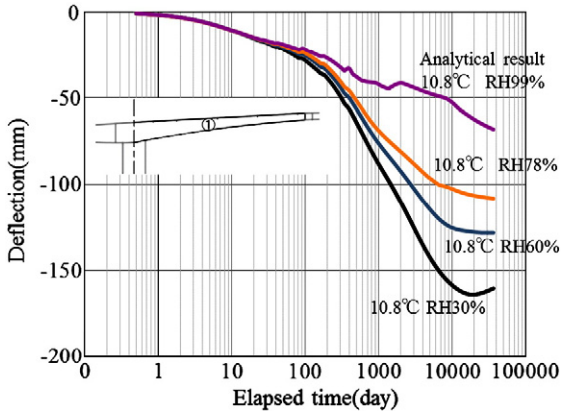

Fig. 8. Variation of deflection with time for relative humidity assumed to be constant.

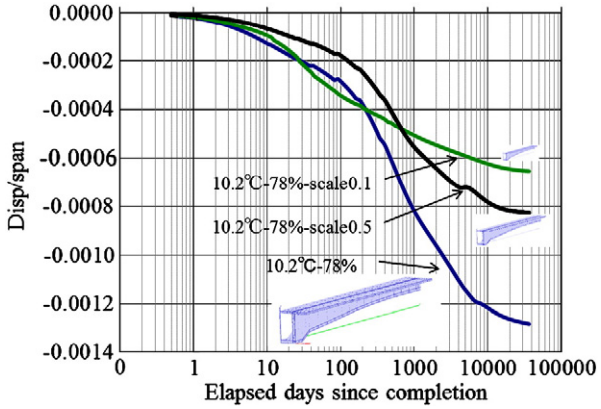

Fig. 10. Variation in deflection with time when the volume to area ratio varies.

at the center of the span (Fig. 8). As the deflection progresses, a distinct difference in the relative humidity between the top and bottom flanges is seen. This is because the box girder top surface was not set as a boundary through which moisture may migrate. The drier the part becomes, the higher the shrinkage, and the faster the progress of the creep. Then, more creep deformation is seen in the bottom flange than in the top one. As a result, the deflection at the center of the span results in excessive deflection. The absolute value of deflection under severe conditions of drying that produce a large gradient in the humidity would be even greater.

In the calculation with the relative humidity fluctuating seasonally (Fig. 9), there is no particular difference compared to the constant humidity over the whole life, and the final values converged to virtually the same displacements. As a time difference can be seen in the variation of the ambient humidity from that of micro-pores in concrete, it is inferred to be the reason why almost no effect of seasonal fluctuation of humidity is brought about.

4.3. Effect of specific surface area of structure

To investigate the effect of specific surface area on the creep deflection, elements with the same shape are magnified or reduced. The effect of self-weight and overlay loads varies in proportion to the 3rd power of the size, the cross-sectional area to resist flexural moment varies in proportion to the 2nd power, and material strength does not depend on dimensions. Therefore, the stress acting on the material varies depending on the structural dimensions. If the stress distribution is different, the creep rate also varies. For investigating the size effect from the thermodynamic point of view, the gravity is applied so as to reproduce the same stress distribution over the different dimensions.

The computed deflection normalized by the span length is shown in Fig. 10. The larger the dimensions are, the more the period at which the deflection accelerates (at several hundred days after start of creep) is delayed. Even though the geometric shape is the same, the drying of the interior of the structure depends on the distance from the surface. The analysis shows that the larger the specific surface area is, the more drying progresses into the interior of the members. It causes the rapid creep deflection.

4.4. Thermodynamic aspects of micro-scale on large-scale actions

The characteristic of the time-dependent constitutive model used in this study is that the hygro-states of moisture trapped in pores in the [nm] to [μm] scales and the macroscopic material behavior are linked. Here, the effect of moisture kept in pores of the microscopic scale on the time-dependent deformation of the large-scale bridge is investigated. Three conditions are set: a) standard, b) capillary tension, which is one of the mechanisms of occurrence of shrinkage, set to be zero at all times, and c) the dashpot, which gives viscosity (component of deformation of gel pores), is numerically frozen in motion. The ambient temperature and the relative humidity are specified to 10.2 °C and 78% respectively, constant throughout the year.

Comparing standard a) with capillary tension zero b) (Fig. 11), it can be seen that a distinct deviation occurs between the two after several tens of days have passed. This indicates that with the progression of drying, the capillary tension contributes a significant

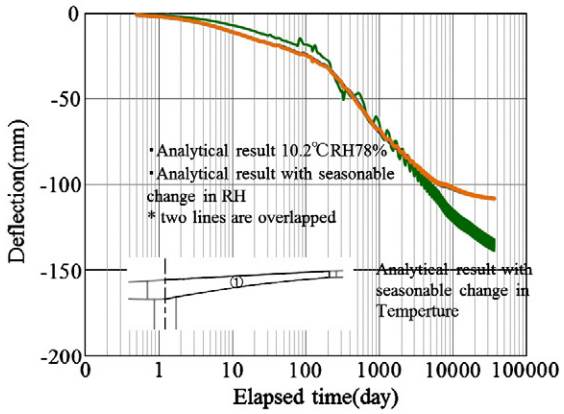

Fig. 9. Variation of deflection with time for relative humidity assumed to fluctuate.

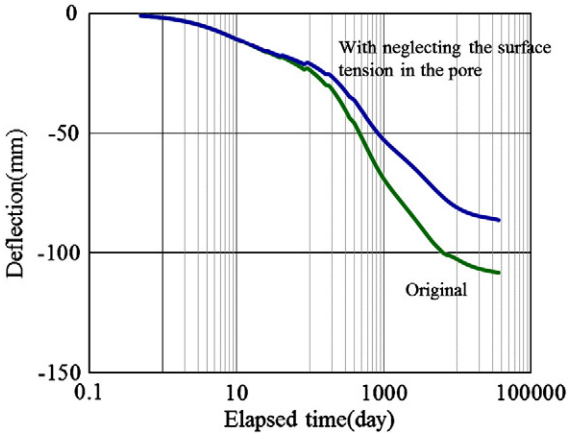

Fig. 11. Effect of movement of water in capillary pores on the structural behavior at the actual structure scale.

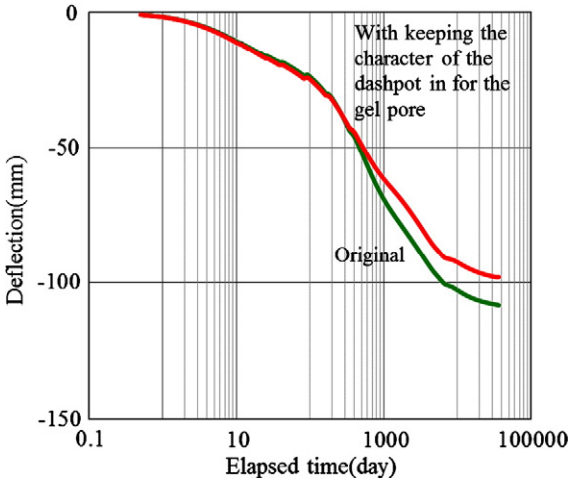

Fig. 12. Effect of the state in the gel pores on the structural behavior at the actual structure scale.

role in the overall behavior of the member. On the other hand, in the case with the gel water stopped c) (Fig. 12) the progress of creep is slower after 1000 days compared with a). This indicates that the sudden increase in deflection after 1000 days is due to the kinematics of moisture in the gel pores. From the above, it can be seen that to predict the structural behavior at the scale of the actual bridge, it is essential to predict the thermodynamic states of moisture at the [nm] scale.

5. Creep deformation of concrete specimens in laboratory

In order to clarify the nonlinearity related to moisture on the structural creep deflection, the authors further conducted the sensitivity analysis for specimen-scale behaviors with which practicing engineers are familiar.

5.1. Analysis outline and conditions

In a concrete test specimen placed in a drying environment, there will be a difference in the moisture states of the surface and the core. It is not a uniform stress or thermodynamic state. The deformation of a concrete test specimen measured in a laboratory is not a material characteristic value, but is just a structural response obtained as the result of thermodynamic events occurring in the microscopic pores. In this analysis system, the material test specimens and full scale structures are similarly dealt with as structures consisting of many finite elements. Therefore, in order to take into account the different thermodynamic states of the surface part and the core, the test specimen is also discretized into finite elements to calculate the deformation. In this chapter, the effect of test specimen size, water-to-cement ratio, and environmental conditions on the "apparent" creep coefficient obtained from standard creep test specimens is investigated.

Taking the standard size of test specimen as a cylinder of diameter 152 mm × height 305 mm, the dimensions of a 4× test specimen were set to diameter 608 mm × height 1220 mm, and for a 1/2 dimension test specimen to diameter 76 mm × height 152.5 mm. Two water-to-cement ratios were investigated: w/c = 39%, which was water-to-cement ratio corresponding to the same materials and composition as

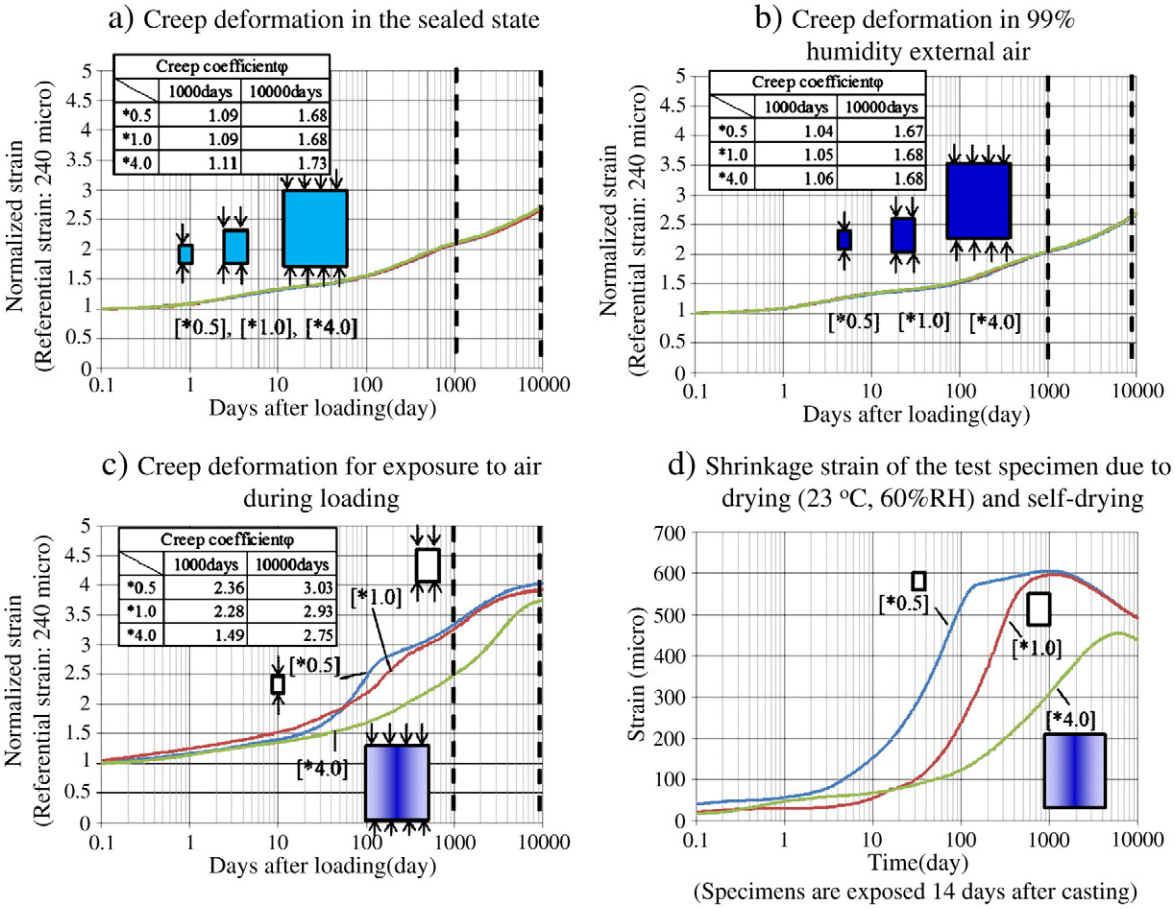

Fig. 13. Variation in creep for different dimensions and w/c = 55%.

Tsukiyono Bridge, and w/c = 55% assuming a normal concrete. At 14 days of age a constant stress was applied, and three environmental conditions were set (from curing to loading sealed conditions were maintained, from curing to loading the external air was a constant 99% relative humidity, and curing was in sealed conditions and from start of loading the specimens were exposed to 23 °C 60% RH air). By reference to many design guides for bridges, the apparent creep coefficient was calculated from the deformation of the test specimens at 3 years. And the vertical axes of the following graphs are normalized by the instantaneous strain produced by the loading.

5.2. Computed creep coefficient

In the case of w/c = 55%, the creep coefficient under the sealed (Fig. 13a)) and humid conditions (Fig. 13b)) are almost the same, and the creep coefficient is calculated to be about 1.1 after 3 years and about 1.6 after 30 years. These computed values agree with the measured ones that have been reported as basic creep in former researches. Under these conditions, size effect is hardly seen, since almost all the pores inside specimens are saturated with condensed water.

On the other hand, creep under the drying condition as shown in Fig. 13c) is computed larger than those under other two cases, which corresponds to well-known phenomena as drying creep. Analytical results prove that the system can automatically simulate both the basic creep and the drying one by only changing thermodynamic boundary conditions. Under drying conditions, the creep coefficient in the 4× case is smaller than the others, because the center of this specimen is harder to be dried by surrounding air when the specimen becomes large. After long term exposure, the shrinkage approaches a maximum, and subsequently a tendency towards recovery is seen. In the analysis, this is attributed to the release of trapped moisture due to the ink bottle effect [17,18].

The results for w/c = 39% are shown in Fig. 14. No difference with dimensions can be seen for the cases where the test specimens are always sealed. This means no size effect on the creep where thermodynamic states are almost uniform in 3D extent. The creep coefficient is calculated to be about 2.1 after 3 years, and about 3.1 after 30 years. On the other hand, in the case with external air humidity 99%, a difference in the creep coefficient from the sealed state is seen, and after 3 years the creep coefficient is about 1.0, and after 30 years about 1.5. In addition, there is a difference depending on the dimensions, in the 4× test specimen the creep coefficient after 3 years is 1.42, and after 30 years is 1.94, a larger value relatively than the others. In the 4× case, as the absolute distance to the center is long, supply of moisture to the center is delayed, which results in a low relative humidity inside the specimen and accelerated creep evolution by Picket effect [15,16]. In other cases, due to the supply of moisture from outside, saturated condition of porous media are always maintained, thereby almost similar creep behaviors are computed.

As shown in Fig. 14c), the creep coefficient under drying condition is similar to that under sealed condition unlike the case of w/c that is 55%. It has also to be noted that the creep coefficient for the 4× specimen in the 99% RH environment is greater than the others, since the moisture profile between the surface and the core is not uniform even under high humid condition. These results clearly indicate that when the w/c is low, self-desiccation inside specimens and corresponding autogenous shrinkage increase [19–23] even if the moisture is not released from the surface of the specimen to the exterior. In

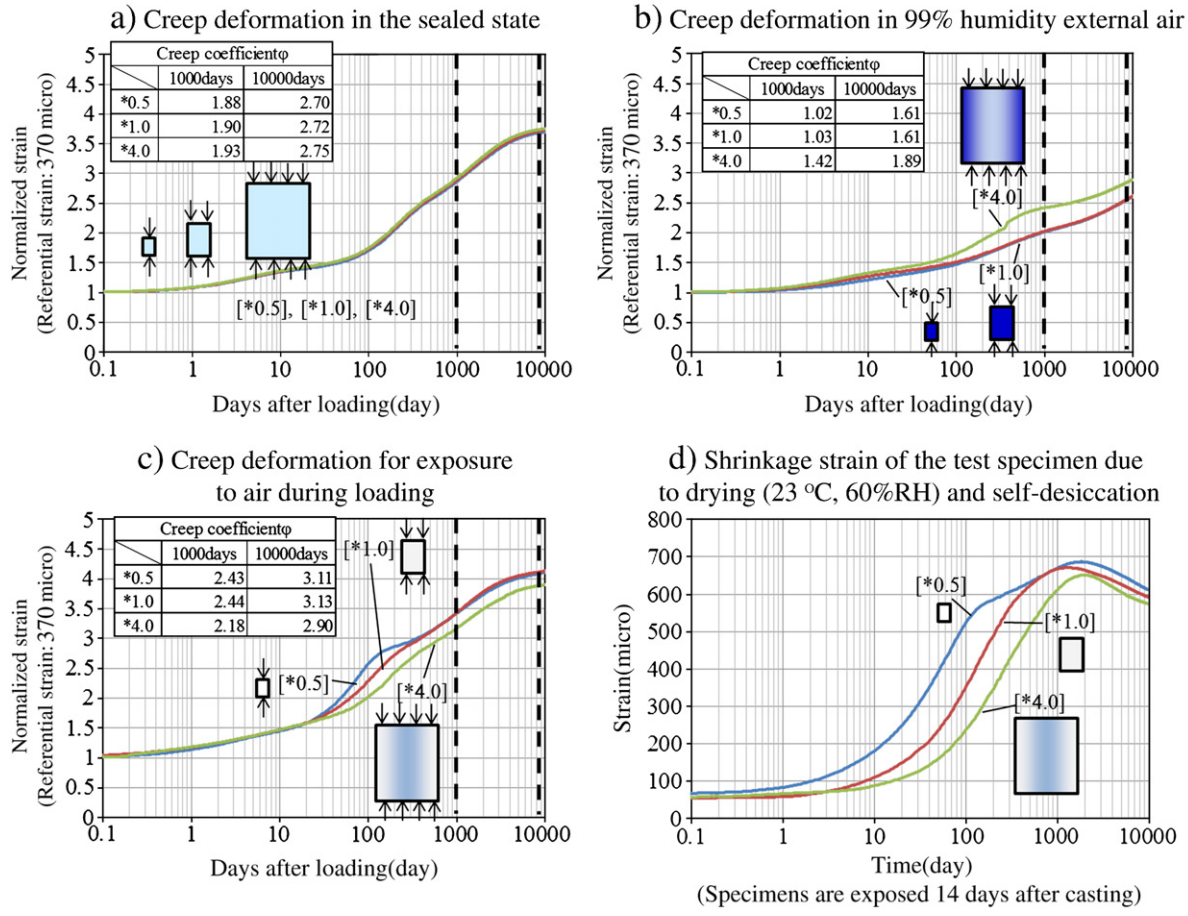

Fig. 14. Variation in creep for different dimensions and w/c = 39% (same composition as Tsukiyono Bridge).

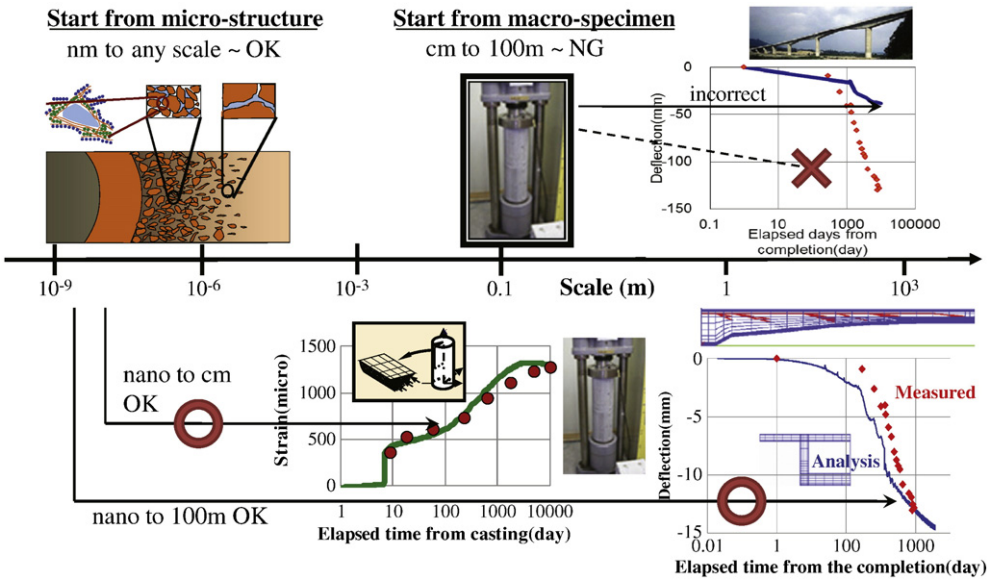

Fig. 15. Multi-scale formation of thermodynamic–mechanistic modeling.

other words, the self-desiccation brings accelerated creep behaviors of low w/c concrete (Picket effect) even under the sealed condition.

The measured basic creep of concrete used in Tsukiyono bridge was reported to be about 1.7 (three-years), which is similar to the simulation results of 1.6 for 99% ambient condition and 2.15 for the sealed one. Then, the multi-scale chemo-physical simulation nearly captures the time dependent behaviors of concrete specimens as well as the real-scale PC girder. However, the linear creep law with the creep coefficient 1.7 could not come up to the large-scale girder as shown in Fig. 15. It is because the loss of condensed moisture by drying (moisture discharged) and/or self-desiccation accelerates the time-dependent deformation of hardened micro cementitious skeleton [24–30] as stated above, and the non-uniform distribution of moisture [29] in space brings about the additional curvature. This effect has been regarded as Picket's effect and indirectly considered by drying creep coefficient or function. This adjustment is thought to hold for the structural members having the similar size of standard test specimens. In other words, this adjustment is definitely size dependent since the drying is much affected by the absolute size. But, the past linear creep law did not treat this size-effect and self-desiccation associated with apparent autogenous shrinkage.

In considering the unavoidable inconsistency of the conventional method, the authors raise the multi-scale modeling as one of promising tools to challenge the problem of excessive deflection of the box-girder PC viaducts, although some unknown factors to be solved in future still exist.

6. Conclusions

The conclusions of this study are as follows.

1) It was possible to closely reproduce the progression of creep deformation measured on an actual bridge using a time-dependent constitutive model taking into consideration the micro-pore structure of the concrete and the state of the moisture in the micro-pores.
2) Creep deformation increases the higher external air temperature. Creep deformation is sensitive to fluctuations in the external air temperature and progresses as an accumulation of the history of relatively high air temperature within the amplitude of the fluctuations.
3) The relative humidity and its distribution within the cross-section affect the creep deformation until it reaches an equilibrium state with the external air. Fluctuations of relative humidity of up to several months have little effect on the amount of creep deformation.
4) The rate of creep varies even if the geometric shape is the same, if the rate of drying varies within the structure due to the dimensions.
5) As a result of calculation that precisely evaluates the effect on the structural behavior of the difference in age due to the construction in stages and the micro-pores, it was predicted that the deflection will converge to about 140–180 mm.
6) It was found from analysis that fixed the various time-dependent models corresponding to the behavior of water in each type of pore that the movement of water in capillaries affects creep deflection from the time of pouring until the relatively short period of time when the water has escaped, and that the cause of the increase in the rate of progression of creep after a certain amount of time has passed after pouring was movement of gel water. Therefore to predict the actual behavior of structures it is essential to take into consideration the coupling between the moisture state at various scales and the mechanical response.
7) The creep deformation mechanisms change depending on the test specimen size, the water cement ratio, and the environmental conditions (sealing, high humidity, in air). In particular, when the water cement ratio is low, the effect of self-drying cannot be ignored.

Acknowledgments

For the analysis of Tsukiyono Bridge, information on the structural parameters and other information from the design stage were provided by Hiroshi Ono, Kazuteru Ueda, and Dr. Eakarat Witchukreangkrai of Shimizu Corporation, for which we wish to express our thanks. This study was carried out with support from the University of Tokyo Global-COE Program for “Sustainable Urban Regeneration”.

References

[1] Y. Hata, N. Oonishi, Y. Watanabe, Creep behavior of prestressed concrete bridge over ten years, Proc. of FIP symposium, 1993, pp. 305–310.
[2] Z.P. Bazant, Q. Yu, G.H. Li, G.J. Klein, V. Kristek, Excessive deflections of record span prestressed box girder, Concrete International, 32, ACI, 2010, No.06.

[3] O. Burdet, Experience in the long-term monitoring of bridges, 3rd fib International Congress, N° 663, Washington D.C., USA, 2010, pp. 108–113.
[4] O. Burdet, M. Baudoux, Long-term deflection monitoring of prestressed concrete bridges retrofitted by external post-tensioning — examples from Switzerland, IABSE Rio 1999, , 1999, Rio de Janeiro, Brazil.
[5] Y. Watanabe, T. Ohura, H. Nishio, M. Tezuka, Practical prediction of creep, shrinkage and durability of concrete in Japan. Creep, shrinkage and durability mechanics of concrete and concrete structures, Proceedings of the CONCREEP 8, CRC Press, 2008, pp. 529–536.
[6] E. Witchukreangkrai, K. Tsuchida, T. Maeda, Y. Watanabe, Long-term deflection monitoring of a cantilever prestressed concrete bridge with intermediate hinges over 25 years. Creep, shrinkage and durability mechanics of concrete and concrete structures, Proceedings of the CONCREEP 8, CRC Press, 2008, pp. 595–600.
[7] Bazant, Z. P. and Baweja, S. (1995): Creep and shrinkage prediction model for analysis and design of concrete structures-ModelB3, Structural Engineering Report 94-10/603c: Northwestern University. Published as draft RILEM recommendation in Materials and Structures (RILEM Paris), 28, 357–365, 415–430, 488–495.
[8] Japan Society of Civil Engineers, Concrete Standard Specification, 1996 edition, 1996 Maruzen.
[9] Japan Society of Civil Engineers, Concrete Standard Specification, 2007 edition, 2007 Maruzen.
[10] K. Maekawa, T. Ishida, T. Kishi, Multi-scale Modeling of Structural Concrete, Taylor & Francis, 2009.
[11] R. Mabrouk, T. Ishida, T. Kishi, K. Maekawa, A unified solidification model of hardening concrete composite for predicting the young age behavior of concrete, Cement and Concrete Composite 26 (2004) 453–461.
[12] S. Asamoto, T. Ishida, K. Maekawa, Time-dependent constitutive model of solidifying concrete based on thermodynamic state of moisture in fine pores, Journal of Advanced Concrete Technology 4 (2) (2006) 301–323.
[13] K. Nakamura, T. Fukuyoshi, M. Moriya, Construction of the Tsukiyono Bridge by the P&Z method, Concrete Journal, 20, JSCE, 1982, No.1.
[14] Japan Meteorological Agency Homepage: http://www.data.jma.go.jp/obd/stats/etrn/index.php
[15] G. Pickett, The effect of change in moisture-content on the creep of concrete under a sustained load, Journal of the ACI 13 (4) (1942) 333–356.
[16] Z. Bazant, L. Panula, Practical prediction of time-dependent deformation of concrete; Part 3 "Drying Creep", Material and Structures 11 (6) (1978) 415–424.
[17] A. Grudemo, Strength–structure relationships of cement paste materials, part 1, Method and basic data for studying phase composition and microstructure, Swedish Cement and Concrete Research Institute, Stockholm, 1997, p. 101, (CBI Research,6,77).
[18] T. Ishida, T. Kishi, K. Maekawa, Enhanced modeling of moisture equilibrium and transport in cementitious materials under arbitrary temperature and relative humidity history, Cement and Concrete Research 37 (2007) 565–578.
[19] E. Tazawa, S. Miyazawa, Autogenous shrinkage caused by self-desiccation in cementitious material, 9th International Congress on the Chemistry of Cement, 4, 1992, pp. 712–718.
[20] T.C. Powers, The mechanics of shrinkage and reversible creep of hardened cement paste, International Conference on the structure of Concrete, Cement and Concrete Association, London, 1965, pp. 319–344.
[21] F.H. Wittmann, Creep and shrinkage mechanisms, in: Bazant, Wittmann (Eds.), Creep and Shrinkage in Concrete Structures, John Wiley & Sons Inc., 1982
[22] H.W. Reinhardt, Autogenous and drying shrinkage of hybrid concrete, Concrete Science and Engineering 4 (14) (2002) 77–83.
[23] E.A.B. Koenders, K. van Breugel, Numerical modeling of autogenous shrinkage of hardening cement paste, Cement and Concrete Research 27 (10) (1997) 1489–1499.
[24] T.C. Powers, The thermodynamics of volume change and creep, Materials and Structures 1 (6) (1968) 487–507.
[25] Z.P. Bazant, Thermodynamics of hindered adsorption and its implications for hardened cement paste and concrete, Cement and Concrete Research 2 (1) (1972) 1–16.
[26] F.H. Wittmann, Surface tension shrinkage and strength of hardened cement paste, Materials and Structures 1 (6) (1973) 547–552.
[27] C.F. Ferraris, F.H. Wittmann, Shrinkage mechanism of hardened cement paste, Cement and Concrete Research 17 (3) (1987) 453–464.
[28] F. Beltzung, F.H. Wittmann, Role of disjoining pressure in cement based materials, Cement and Concrete Research 35 (12) (2005) 2364–2370.
[29] A. Hillerborg, A modified absorption theory, Cement and Concrete Research 15 (1985) 809–816.
[30] S. Nagataki, A. Yonekura, The mechanism of drying shrinkage and creep of concrete, Concrete Library International, JSCE, 1984, No.3.
[31] K. Maekawa, T. Ishida, T. Kishi, Multi-scale modeling of concrete performance — integrated material and structural mechanics, Journal of Advanced Concrete Technology 1 (2) (2003) 91–126.
[32] E. Gebreyouhannes, K. Maekawa, Numerical simulation on shear capacity and post-peak ductility of reinforced high-strength concrete coupled with autogenous shrinkage, Journal of Advanced Concrete Technology 9 (1) (2011) 73–88.
[33] P.O. Iqbal, T. Ishida, Modeling of chloride transport coupled with enhanced moisture conductivity in concrete exposed to marine environment, Cement and Concrete Research 39 (4) (2009) 329–339.